



# A Nanospherical Metal–Organic Framework UiO-66 for Solid-Phase Microextraction of Polycyclic Aromatic Hydrocarbons

Yu Tian<sup>1</sup> · Min Sun<sup>1</sup> · Xiuqin Wang<sup>1</sup> · Chuannan Luo<sup>1</sup> · Juanjuan Feng<sup>1</sup>

Received: 2 January 2018 / Revised: 16 April 2018 / Accepted: 18 April 2018 / Published online: 24 May 2018  
© Springer-Verlag GmbH Germany, part of Springer Nature 2018

## Abstract

Polycyclic aromatic hydrocarbons are a low content, but highly toxic organic pollutant in the environment. Because of their great threat to the health and survival of humans and other creatures, it is necessary to have a very simple and convenient as well as highly sensitive method to detect them. Based on previous studies, a nanospherical metal–organic framework UiO-66 was re-applied as the solid-phase microextraction coating and the extraction performance of polycyclic aromatic hydrocarbons was investigated. Scanning electron microscope and X-ray diffraction were used to characterize the extraction material. The extraction conditions were optimized factor by factor, and the analytical method was established with broad linear ranges (0.03–50 and 0.10–50  $\mu\text{g L}^{-1}$ ), excellent correlation coefficients (0.9955–0.9993) and low limits of detection (0.01–0.03  $\mu\text{g L}^{-1}$ ). The analytical method was applied to detect polycyclic aromatic hydrocarbons in rainwater and lake water, and satisfactory results were obtained. Compared with previous reports, this method had wider linear range, lower limit of detection and longer service life.

**Keywords** Solid-phase microextraction · Polycyclic aromatic hydrocarbons · Metal–organic frameworks · Nanospherical UiO-66 · Environmental analysis

## Introduction

Polycyclic aromatic hydrocarbons (PAHs) are produced mostly due to the incomplete combustion of carbon-containing substance [1], and some of them are a class of carcinogens. They had been listed as priority pollutants by the US Environmental Protection Agency [2]. Human beings are exposed to PAHs primarily through contact with air and intake of water and food [3], and high toxicity makes PAHs a serious threat. PAHs are widely distributed in the environment, but it is difficult to detect them due to the very low content and the complexity of the sample matrix [4]. Therefore, effective separation and enrichment are essential in the analysis of the actual sample. Sample preparation technology has become the most critical issue in the analysis process. Conventional methods have shortcomings including

cumbersome operation, low sensitivity and poor selectivity [5]. Solid-phase microextraction (SPME), introduced by Pawliszyn in the 1990s [6], is replacing traditional technology, due to its advantages of simple operation, solvent-free nature, sensitivity and quickness [7]. It has been widely applied in environmental testing [8–10], food analysis [11, 12], biological analysis [13, 14], pesticide residues [15, 16], drug monitoring [17] and other fields. Fluorinated polyaniline was used as an SPME coating for PAHs by Li's group [18]. A variety of PAHs have been successfully detected in the analysis of rainwater and lake water. Titanium dioxide nanosheet coating functionalized with phenyl group was fabricated on a titanium wire as an SPME fiber for PAHs by Guo et al. [19]. It was used for the detection of PAHs in rainwater and poly-river water, and multiple analytes were quantified. Yang et al. used the electrodeposition method to self-assemble poly(3,4-ethylenedioxythiophene)@gold nanoparticles on stainless steel wires as the SPME fiber for PAHs [20]. The analytical method was built for the detection of PAHs in real samples of lakes, rain and soil, and some analytes were detected successfully. These results again prove the persistency of PAHs. Therefore, it is evident

✉ Juanjuan Feng  
chm\_fengjuanjuan@ujn.edu.cn

<sup>1</sup> Key Laboratory of Interfacial Reaction and Sensing Analysis in Universities of Shandong, School of Chemistry and Chemical Engineering, University of Jinan, Jinan 250022, People's Republic of China

that the pollution in rainwater and lakes caused by PAHs deserves more attention.

The extractive coating is the most critical component of the SPME fiber. The extraction performance depends on the coating material, and different physical structure can also improve its extraction property, for example, nanomaterials provide larger specific surface area [21]. The material with excellent adsorptive properties and a large surface area is the best choice for SPME coating. Metal–organic frameworks (MOFs), in which metal ions are linked together by organic bridging ligands [22], have been widely researched in catalysis [23, 24], gas storage [25, 26], drug delivery [27, 28] and separation [29, 30] due to their intriguing properties such as a highly ordered three-dimensional framework structure, large accessible surface area, controlled porosity, and tunable chemical properties [31, 32]. These specific properties allow MOFs to be employed as an SPME coating, and they have broad development potential.

UiO-66 is an MOF formed by the combination of terephthalic acid and zirconium, and some studies have reported that it has good adsorption properties [33, 34]. Shang's group introduced UiO-66 into the SPME field by the physical coating method, and phenols were used as the targets to investigate the extraction performance [33]. A few years later, Gao's group synthesized UiO-66 on silica fiber in situ and used it for the extraction of PAHs [34]. The results showed that the extraction performance of the latter study was better. However, the silica fiber is fragile and not conducive to long-term use. In this work, the stainless steel wire instead of silica fiber has been used as a substrate to improve the mechanical strength. Nanospherical UiO-66 has been synthesized with increased specific surface area and hydrophobicity, which can be more conducive to extract hydrophobic PAHs. MOFs can provide more sites for adsorption, and the state of nanospheres can also change the hydrophobicity of the material, which makes it easier to extract the hydrophobic analytes.

## Experimental

### Materials and Reagents

The stainless steel wire ( $\Phi=0.3$  mm) was purchased from Shanghai Gauge Industry and Trade Co., Ltd (Shanghai, China). Hydrochloric acid (36%) was obtained from Laiyang City Kant Chemical Co., Ltd (Laiyang, Shandong, China). Terephthalic acid was available from Alfa Aesar (Ward Hill, USA). Zirconium tetrachloride was obtained from Tianjin Ke Miou Chemical Reagent Co., Ltd (Tianjin, China). Acetic acid as well as potassium chloride was from the National Pharmaceutical Group Chemical Reagent Co., Ltd (Shanghai, China). *N,N*-Dimethylformamide (DMF) was obtained

from Guangzhou Guanghua Chemical Co., Ltd (Guanghua, Guangzhou, China). The silicone sealant was purchased from American Car Co., Ltd (Indiana, USA). Methanol was bought from Tianjin Fuxu Fine Chemical Co., Ltd (Tianjin, China). Naphthalene (Nap), acenaphthylene (Acy), acenaphthene (Ace), fluorene (Flu), phenanthrene (Phe), anthracene (Ant), fluoranthene (Flour), pyrene (Py) and chrysene (Chr) were available from Shanghai Pure Reagent Co., Ltd (Shanghai, China).

### Apparatus

An Agilent 7890A GC system (Agilent Technologies, USA) equipped with a flame ionization detector (FID) and a split/splitless inlet was employed to analyze samples. HP-5 capillary column (30 m  $\times$  0.32 mm i.d.  $\times$  0.25  $\mu$ m film thickness) was applied for the separation. The carrier and make-up gas were all ultrapure nitrogen (> 99.999%) and were set at 3 and 25 mL min<sup>-1</sup>, respectively. The inlet was kept at 300 °C to allow the analyte to fully vaporize and used with the splitless injection mode. The detector temperature was fixed at 300 °C. To achieve rapid and simultaneous detection, the oven temperature was programmed as follows: the initial temperature was set at 100 °C and programmed at 10 °C min<sup>-1</sup> to 300 °C, and the process needed 20 min.

Scanning electron microscope (SEM) (SUPRATM55, Carl Zeiss AG, Oberkochen, Germany) was used to characterize the surface morphology of the SPME fiber. X-ray diffraction (XRD) was performed using a D8 FOCUS diffractometer (Bruker-AXS, Germany) with Cu K $\alpha$  radiation.

### Preparation of SPME Fiber

One end (4 cm length) of the stainless steel wire was etched in hydrochloric acid (36%) for 2.5 h, then it was ultrasonically cleaned for 5 min with ultrapure water. After that, the stainless steel wire with a rough surface and smaller diameter was obtained, which was easy to be coated and not easily scratched.

Nanospherical UiO-66 was prepared by a modified synthesis method according to the previous literature [35], and some steps were changed to obtain uniform nanoparticles. Briefly, zirconium tetrachloride (0.400 g, 1.70 mmol) and 0.6 mL of the templating agent (acetic acid) were dissolved in 40 mL of DMF. After mixing evenly, 0.285 g terephthalic acid was added. Ultrasound was carried out for 5 min to make the solution uniform. The reaction solution was put in an autoclave and heated at 120 °C for 24 h. The reaction solution was centrifuged and the precipitate was washed three times with DMF solvent to obtain a white crystalline product. Then, the product was washed three times with methanol and lyophilized for 20 h. The obtained solid powder was ground and was then adhered to the treated end of

the stainless steel wire with silicone sealant. The length of the coating was controlled at about 3.5 cm.

## Sample Preparation

A PAHs (Nap, Acy, Ace, Flu, Phe, Ant, Flour, Py and Chr) solution with a concentration of  $100 \text{ mg L}^{-1}$  was prepared with methanol and stored in a refrigerator at  $4^\circ\text{C}$ . The working solution was prepared daily by diluting the above solution with ultrapure water to  $10 \mu\text{g L}^{-1}$ . Rainwater and lake water were collected as the actual samples.

## Solid-Phase Microextraction Procedure

The prepared fiber was inserted into a  $5 \mu\text{L}$  micro-syringe to assemble into an SPME device. Before extraction, the fiber was inserted into an inlet at  $300^\circ\text{C}$  for 15 min to treat the coating, which made the coating indurated. All extractions were carried out in a 10 mL sample solution through a direct immersion mode. After the extraction, the fiber was pulled back into the syringe, which can reduce the loss of analytes during the transfer process. Subsequently, the syringe was quickly inserted into a GC inlet of  $300^\circ\text{C}$ , the fiber was

pushed out and the analytes were desorbed. About 4 min later, the syringe was pulled out. To prevent the residual effect on the next test, the syringe was desorbed for another 5 min in the inlet. Each data point in this experiment was repeated three times.

## Results and Discussion

### Characterization of Extraction Coating

The morphology of the coating was characterized by SEM. As shown in Fig. 1a, the coating is evenly covered on the surface of the stainless steel wire. Figure 1b is an SEM image observed at a higher magnification, and the coating material is presented as a nanoscale ball with uniform particle size. These nanospheres can greatly increase the specific surface area and thus effectively enhance the extraction efficiency. As can be seen from the cross section of the fiber in Fig. 1c, the coating thickness can be measured to about  $8.5 \mu\text{m}$ . The coating material was characterized by XRD, and the spectrum is shown in Fig. 1d. The spectrum is in good agreement with the standard XRD spectrum of

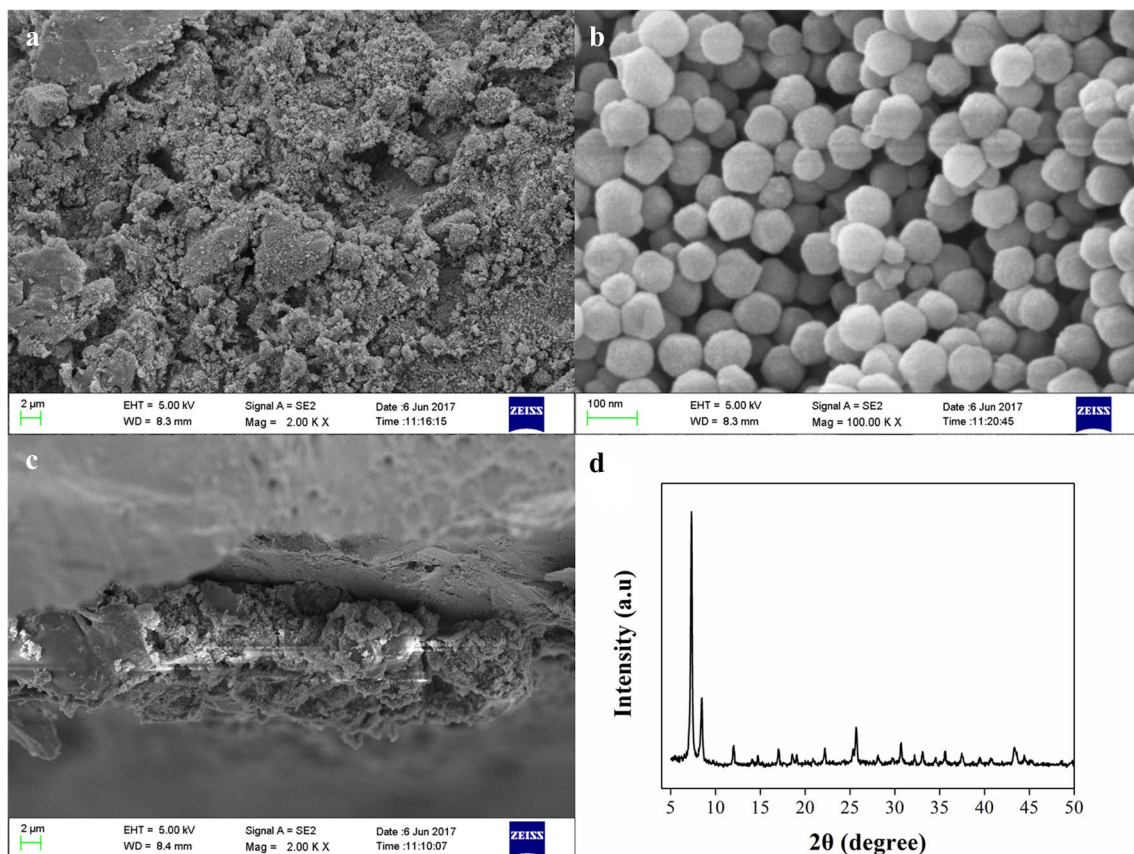


**Fig. 1** SEM images and XRD spectrum of coating materials and fibers. **a, b** The fiber surface, **c** the cross section of fiber and **d** the XRD spectrum of the coating material

UiO-66, which proves that the synthesized nanospheres are the metal organic skeleton of zirconium.

## Optimization of Extraction Conditions

The perfect extraction procedure needs to be carried out under optimal extraction conditions. The most important factors affecting the extraction efficiency were investigated and these are extraction temperature, extraction time, ionic strength of sample solutions and stirring rate.

### Extraction Temperature

It is well known that the increase in temperature promotes the movement of molecules and is beneficial for the rapid completion of the extraction process. However, since most of the adsorption is exothermic, the temperature rise will be detrimental to the distribution equilibrium according to Le Chatelier's principle. That is to say that the effect of temperature rise on the extraction efficiency is both negative and positive, so there will be an optimal temperature.

The effect of temperature on extraction efficiency starts at an ambient temperature of 25 °C. As shown in Fig. 2a, the peak areas which represent the extraction efficiency increase significantly from 25 to 30 °C. However, when the temperature exceeds 30 °C, the peak areas decrease to a different degree as the temperature increases. The increase in peak areas results from the effect of temperature on molecular motion over the effect of temperature on the distribution equilibrium, so the positive effect is greater than the negative effect and vice versa. In summary, the largest peak areas are obtained at 30 °C, and this was selected as the optimum extraction temperature to get the maximum extraction efficiency.

### Extraction Time

Extraction time is one of the key factors affecting the extraction efficiency. The distribution equilibrium can be achieved if the extraction time is sufficient. If the extraction time is too short, low extraction efficiency will be obtained on account of the extraction not being balanced. When the extraction time is sufficient, the extraction equilibrium can

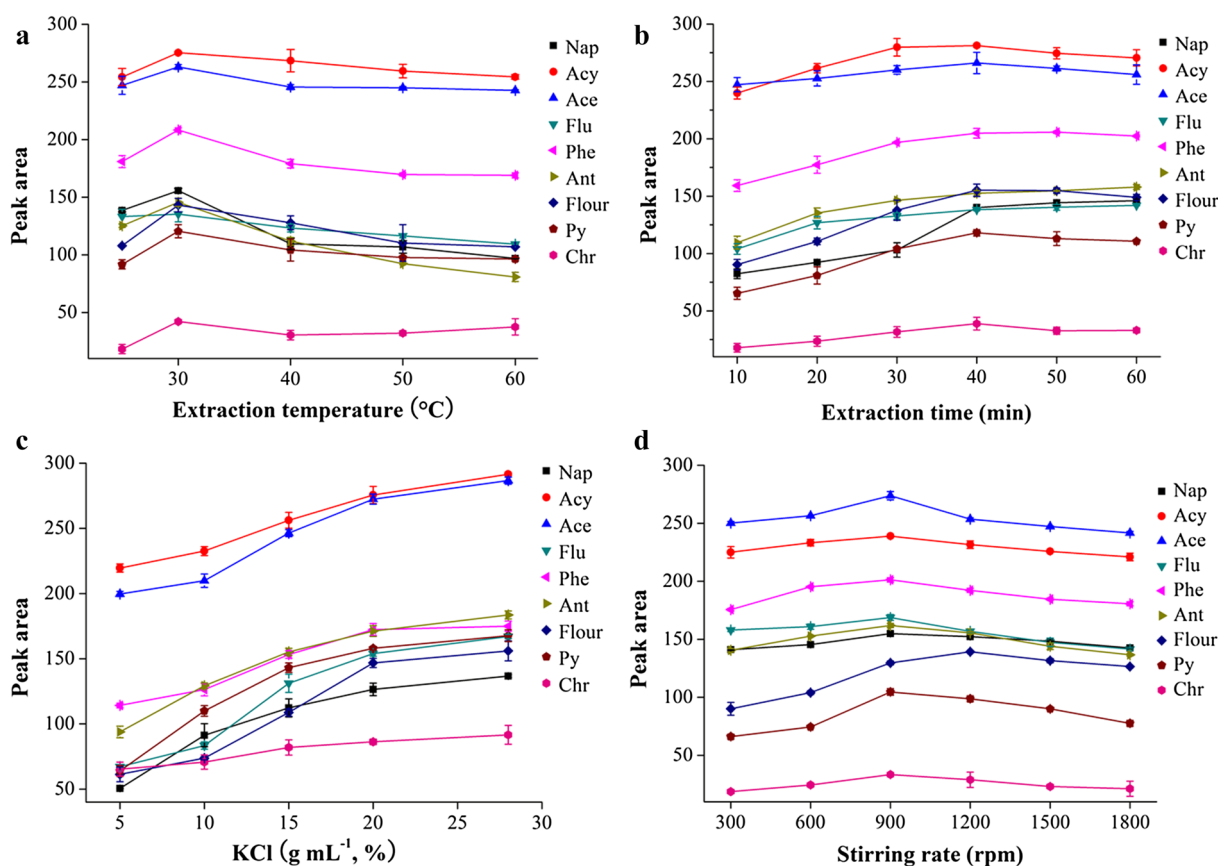


**Fig. 2** The influence of different factors on the extraction efficiency. **a** Extraction temperature, **b** extraction time, **c** ionic strength of sample solutions and **d** stirring rate. Conditions: the concentration of analytes

in the working solution, 10  $\mu\text{g L}^{-1}$ ; each data point was average value of parallel determination three times

be achieved and the coating will not continue to extract the analytes. Hence, when the peak areas no longer increase exactly, the distribution equilibrium has been reached and the time is the optimum extraction time.

From 10 to 60 min, the effect of extraction time on extraction efficiency was investigated. It can be seen from Fig. 2b that the peak area of each analyte increases from 10 to 40 min. When the extraction time exceeds 40 min, the peak areas no longer increase. To achieve maximum extraction efficiency while saving time, 40 min was selected as the optimal extraction time.

### Ionic Strength of Sample Solutions

After the addition of the electrolyte to the aqueous solution, the solubility of other electrolytes and non-electrolytes in the solution decreases and increases accordingly, known as the salting-out and salt-soluble effects. PAHs are non-electrolytes. When the electrolyte is added to the solution, it competes with solvent molecules. Electrolyte ions compete with solvent molecules strongly, which will lead to the solvent molecules migrating from the non-electrolyte to the electrolyte ion, thereby reducing the non-electrolyte hydration and solubility. So, the addition of electrolyte in solution can decrease the solubility of PAHs and increase their concentration in the coating.

The effect of ionic strength on the extraction efficiency was studied by dissolving different contents of KCl in the solution. Due to the limited solubility of KCl, the effect of ionic strength on extraction efficiency was investigated from 5% (g mL<sup>-1</sup>) to 28% KCl. As shown in Fig. 2c, all peak areas increase to varying degrees with the increase in salt content. To obtain the highest extraction efficiency, 28% KCl was added to every solution.

### Stirring Rate

Effective agitation to the extraction solution accelerates the movement of the molecule, thereby promoting the adsorption of the analytes. However, if the stirring speed increases sharply, bubbles and vortices that appear inside the solution greatly shrink the contact area between the solution and the coating, eventually leading to a sharp decline of the extraction efficiency. The increase in the stirring rate has both beneficial and detrimental effects on the extraction efficiency, and so optimization of the stirring rate is very necessary.

The stirring rate was optimized from 300 to 1800 rpm, and a rate point was determined every 300 rpm. As shown in Fig. 2d, the peak areas increase to varying degrees with increase in the rate from 300 to 900 rpm. When the agitation rate exceeds 900 rpm, all of the peak areas except for Ace start decreasing. Combined with the previous description, 900 rpm was selected as the optimal stirring rate.

### Optimization of Desorption Time

A sufficient desorption time allows the analytes to be desorbed completely and all the analytes can be accurately detected. Too short a desorption time not only fails to provide accurate results, but also affects the next test due to the residual effect. It is worth noting that a long period of high temperature may cause damage to the coating, so it is necessary to study and get the best desorption time.

The effect of desorption time on the extraction efficiency was researched from 1 to 5 min. It can be seen obviously from Fig. 3 that the peak areas increase with the increase of desorption time before 3 min. When the desorption time increases from 3 to 4 min, the peak areas of most analytes no longer increase except for Acy, Ace and Chr. All peak areas achieve a balance after 4 min, which means all the analytes have been completely desorbed. In summary, 4 min was selected as the optimum desorption time.

### Method Evaluation

Under optimal conditions, the analytical method was established by extracting a series of standard solutions with different concentrations. The results of the analytical method, including linear range, correlation coefficient, limit of quantitation (LOQ), limit of detection (LOD) and repeatability are listed in Table 1. The linear ranges are 0.10–50 µg L<sup>-1</sup> for Nap and Chr, and the linear ranges for others analytes are 0.03–50 µg L<sup>-1</sup>. The correlation coefficients are in the range of 0.9955–0.9993. The LOQs for analytes range from 0.03 to 0.10 µg L<sup>-1</sup>. The LODs were investigated by extracting distilled water that spiked at various grades to obtain a signal based on three times signal-to-noise ratios. The LODs of the analytes are in the range of 0.01–0.03 µg L<sup>-1</sup>. The intra-fiber

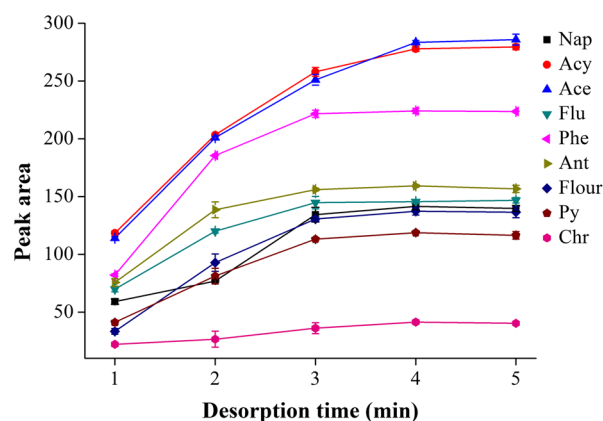


**Fig. 3** The optimization of desorption time. Conditions: extraction temperature, 30 °C; extraction time, 40 min; content of KCl, 28% (w/v); stirring rate 900 rpm; the concentration of analytes in the working solution, 10 µg L<sup>-1</sup>; each data point was average value of parallel determination three times

**Table 1** Analytical performances of the SPME–GC method

Analytes	Linear range ( $\mu\text{g L}^{-1}$ )	Correlation coefficient ( $R$ ) <sup>a</sup>	LOQs ( $\mu\text{g L}^{-1}$ )	LODs ( $\mu\text{g L}^{-1}$ )	Repeatability ( $n=5$ , RSD%) <sup>b</sup>	
					Intra-fiber	Inter-fiber
Nap	0.10–50	0.9977	0.10	0.03	0.4	0.9
Acy	0.03–50	0.9983	0.03	0.01	1.8	2.1
Ace	0.03–50	0.9961	0.03	0.01	2.7	2.7
Flu	0.03–50	0.9993	0.03	0.01	0.6	0.7
Phe	0.03–50	0.9991	0.03	0.01	1.3	1.5
Ant	0.03–50	0.9961	0.03	0.01	0.1	0.4
Flour	0.03–50	0.9986	0.03	0.01	3.3	4.0
Py	0.03–50	0.9982	0.03	0.01	4.7	5.6
Chr	0.10–50	0.9955	0.10	0.03	3.9	4.1

<sup>a</sup>Calibration level:  $n=10$ <sup>b</sup>Spiked level:  $10 \mu\text{g L}^{-1}$ 

repeatability was researched under the same conditions, and RSD was less than 4.7%. The inter-fiber repeatability was investigated with five fibers, and the RSD was less than 5.6%. The values of RSD obtained by this method are much better than those obtained by solid-phase extraction or liquid–liquid extraction. It also demonstrated that SPME was better than traditional extraction methods.

The proposed method is compared with the related reports and the results are shown in Table 2. Shang's group used the UiO-66 coating for extracting phenols. Phenols are hydrophilic and the extraction sensitivity is low; relatively speaking, nanospherical UiO-66 has higher sensitivity for PAHs. The enhancement factor was based on the ratio of the concentration of the analyte extracted by the coating to the concentration of the analyte in the working solution. They are in the range of 1051–3966, higher than that of a previous study, 152–3819. Gao's group synthesized UiO-66 in situ on the surface of silica fiber; however, the silica fiber is fragile and is not conducive for use. Stainless steel wire was used as a carrier to replace the silica fiber, and excellent extraction performance was obtained while the service life was also improved. From the overall results, nanospherical UiO-66 as SPME coating shows excellent performance for PAHs.

## Application to Real Samples

To evaluate the performance of the established analytical method for PAHs in real samples, rainwater and lake water were analyzed. The chromatograms for detecting rainwater and lake water are presented in Fig. 4a, b, respectively. As listed in Table 3, the concentrations of Ace, Ant, Py and Chr are detected to be 1.34, 0.87, 1.28 and  $3.36 \mu\text{g L}^{-1}$  in rainwater. Nap and Flour are also detected, but they are not quantified because the contents are very low and not within the limit of quantitation. Acy, Flu and Phe are not detected in rainwater. The recoveries of the analytes range from 81.4 to 118% when the spiked level in rainwater is  $5 \mu\text{g L}^{-1}$ , and range from 84.4 to 108% when the spiked level is  $10 \mu\text{g L}^{-1}$ . In lake water, the concentrations of Nap, Py and Chr are detected to be 0.56, 2.25 and  $3.18 \mu\text{g L}^{-1}$ . Phe and Flour are also successfully detected, but are not quantified. The other analytes are not detected. The recoveries range from 80.2 to 115% when the spiked level in the lake water is  $5 \mu\text{g L}^{-1}$ , and from 85.1 to 109% when the spiked level is  $10 \mu\text{g L}^{-1}$ . Limits for the PAH concentration from the National Recommended Water Quality Criteria of the USEPA [36], the European Council Directive [37] and the Canadian environmental

**Table 2** Comparison of the extraction performance of different fibers made by UiO-66

Coating	Analytical method	Coating preparation method	Analytes	Life-time (times)	Linear range ( $\mu\text{g L}^{-1}$ )	LOD ( $\text{ng L}^{-1}$ )	EFs	References
UiO-66	GC	Glued to stainless steel wire with epoxy resin glue	Phenols	–	1–1000	110–1230	152–3819	[30]
UiO-66	GC–MS	Synthesized in situ on fused-silica fibers	PAHs	90	0.001–5	0.28–0.60	–	[31]
Nano-spherical UiO-66	GC	Glued to stainless steel wire with silicone sealant	PAHs	120	0.03–50	10–30	1051–3966	This work

quality guidelines [38] are specified in Table 4. On comparing the data in Tables 3 and 4, most of the analytes did not exceed the specified levels, but very few analytes exceeded the specified levels.

## Conclusion

A nanospherical metal–organic framework UiO-66 was prepared as the coating for SPME fiber. Series PAHs were employed as simulate analytes to study the extraction performance of the fiber. The extraction conditions were optimized and the analytical method was established coupled with GC. Although the results shown in Table 3 and Fig. 4 are quite satisfactory, there are two analytes (Py, Chr) in the real sample that are over the limits of the concentration standards

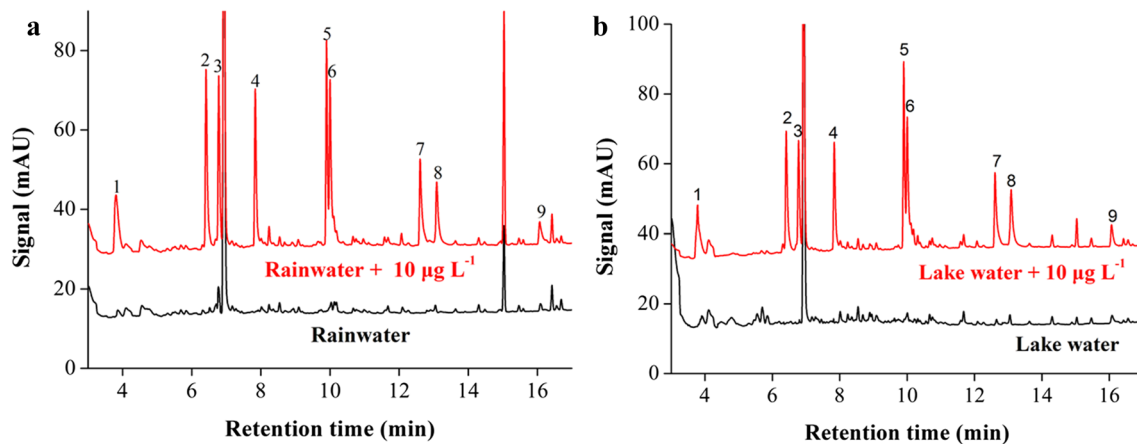


**Fig. 4** The chromatograms for rainwater (a) and lake water (b). (1) Nap, (2) Acy, (3) Ace, (4) Flu, (5) Phe, (6) Ant, (7) Flour, (8) Py, (9) Chr. Conditions: extractin temperature, 30 °C; extraction time, 40 min; content of KCl, 28% (w/v); stirring rate, 900 rpm; desorption time, 4 min

**Table 3** The detected results and recoveries for PAHs in the actual samples

Analytes	Rainwater ( $\mu\text{g L}^{-1}$ , $n=3$ )	Recovery ( $n=3$ , %) <sup>a</sup>	Recovery ( $n=3$ , %) <sup>b</sup>	Lake water ( $\mu\text{g L}^{-1}$ , $n=3$ )	Recovery ( $n=3$ , %) <sup>a</sup>	Recovery ( $n=3$ , %) <sup>b</sup>
Nap	N.Q	91.2 ± 1.92	86.4 ± 2.01	0.56	97.4 ± 5.16	87.7 ± 2.65
Acy	N.D	87.8 ± 3.08	95.6 ± 7.51	N.D	104.3 ± 7.65	93.6 ± 1.61
Ace	1.34	93.8 ± 0.56	93.9 ± 1.10	N.D	86.2 ± 4.08	96.8 ± 4.91
Flu	N.D	81.7 ± 0.28	96.0 ± 6.49	N.D	87.3 ± 0.08	96.0 ± 2.16
Phe	N.D	85.4 ± 4.31	95.5 ± 5.68	N.Q	92.4 ± 2.66	91.2 ± 2.13
Ant	0.87	96.1 ± 2.56	87.6 ± 0.18	N.D	113 ± 1.52	98.1 ± 1.16
Flour	N.Q	97.5 ± 9.22	99.7 ± 4.27	N.Q	83.8 ± 3.56	101 ± 6.17
Py	1.28	92.1 ± 2.02	92.3 ± 1.86	2.25	86.7 ± 3.12	93.1 ± 6.05
Chr	3.36	112 ± 6.16	105 ± 3.42	3.18	107 ± 0.82	108 ± 1.14

N.D not detected, N.Q detected, but not quantified

<sup>a</sup>Spiked level: 5  $\mu\text{g L}^{-1}$

<sup>b</sup>Spiked level: 10  $\mu\text{g L}^{-1}$

**Table 4** Surface water PAH concentration standards ( $\mu\text{g L}^{-1}$ )

Country/organization	Nap	Acy	Ace	Flu	Phe	Ant	Flour	Py	Chr
USA	–	70	70	50	–	300	20	20	0.12
European Union	2.4	–	–	–	–	0.1	0.1	–	–
Canada	1.1	5.8	5.8	3	0.4	0.01	0.04	0.03	–

(0.03  $\mu\text{g L}^{-1}$ , 0.12  $\mu\text{g L}^{-1}$ ); their study could be interesting for further research. The fibers have a good extraction performance for PAHs due to the hydrophobic and  $\pi$ - $\pi$  interactions between PAHs and the UiO-66 framework.

**Acknowledgements** The authors would like to thank the Shandong Provincial Natural Science Foundation of China (no. ZR2017MB043) and the National Natural Science Foundation of China (NSFC, nos. 21777054 and 21405061) for the support to this study.

## Compliance with Ethical Standards

**Conflict of interest** The author declares that he has no conflict of interest.

**Ethical approval** This article does not contain any studies with human participants or animals performed by the authors.

## References

- Wenzl T, Simon R, Anklam E, Kleiner J (2006) Analytical methods for polycyclic aromatic hydrocarbons (PAHs) in food and the environment needed for new food legislation in the European Union. *Trend Anal Chem* 25:716–725
- Liu Y, Zhou J, Zhao R, Chen X (2012) Using Zn/Al layered double hydroxide as a novel solid-phase extraction adsorbent to extract polycyclic aromatic hydrocarbons at trace levels in water samples prior to the determination of gas chromatography-mass spectrometry. *Anal Bioanal Chem* 404:1603–1610
- Sun M, Feng J, Qiu H, Fan L, Li L, Luo C (2013) A solid-phase microextraction fiber with carbon nanoparticles as sorbent material prepared by a simple flame-based preparation. *J Chromatogr A* 1300:173–179
- Zhang G, Zang X, Li Z, Wang C, Wang Z (2014) Polydimethylsiloxane/metal-organic frameworks coated fiber for solid-phase microextraction of polycyclic aromatic hydrocarbons in river and lake water samples. *Talanta* 129:600–605
- Speltini A, Scalabrini A, Maraschi F, Sturini M, Profumo A (2017) Newest applications of molecularly imprinted polymers for extraction of contaminants from environmental and food matrices: a review. *Anal Chim Acta* 974:1–26
- Arthur CL, Pawliszyn J (1990) Solid phase microextraction with thermal desorption using fused silica optical fibers. *Anal Chem* 62:2145–2148
- Hu X, Liu C, Li J, Luo R, Jiang H, Sun X, Shen J, Han W, Wang L (2017) Hollow mesoporous carbon spheres-based fiber coating for solid-phase microextraction of polycyclic aromatic hydrocarbons. *J Chromatogr A* 1520:58–64
- Ma M, Wang H, Zhen Q, Zhang M, Du X (2017) Development of nitrogen-enriched carbonaceous material coated titania nanotubes array as a fiber coating for solid-phase microextraction of ultraviolet filters in environmental water. *Talanta* 167:118–125
- Wang H, Song W, Zhang M, Zhen Q, Guo M, Zhang Y, Du X (2016) Hydrothermally grown and self-assembled modified titanium and nickel oxide composite nanosheets on Nitinol-based fibers for efficient solid phase microextraction. *J Chromatogr A* 1468:33–41
- Raza W, Mei X, Wei Z, Ling N, Yuan J, Wang J, Huang Q, Shen Q (2017) Profiling of soil volatile organic compounds after long-term application of inorganic, organic and organic-inorganic mixed fertilizers and their effect on plant growth. *Sci. Total Environ* 607:339–350
- Al-Alam J, Fajloun Z, Chbani A, Millet M (2017) A multiresidue method for the analysis of 90 pesticides, 16 PAHs, and 22 PCBs in honey using QuEChERS-SPME. *Anal Bioanal Chem* 409:5157–5169
- Ji J, Liu H, Chen J, Zeng J, Huang J, Gao L, Wang Y, Chen X (2012) ZnO nanorod coating for solid phase microextraction and its applications for the analysis of aldehydes in instant noodle samples. *J Chromatogr A* 1246:22–27
- Zeng J, Chen J, Li M, Subhan F, Chong F, Wen C, Yu J, Cui B, Chen X (2015) Determination of amphetamines in biological samples using electro enhanced solid-phase microextraction-gas chromatography. *J Chromatogr B* 1000:169–175
- Hou X, Wang L, Guo Y (2017) Recent developments in solid-phase microextraction coatings for environmental and biological analysis. *Chem Lett* 46:1444–1455
- Gómez-Ríos GA, Gionfriddo E, Poole J, Pawliszyn J (2017) Ultrafast screening and quantitation of pesticides in food and environmental matrices by solid-phase microextraction-transmission mode (SPME-TM) and direct analysis in real time (DART). *Anal Chem* 89:7240–7248
- Xie L, Liu S, Han Z, Jiang R, Zhu F, Xu W, Su C, Ouyang G (2017) Amine-functionalized MIL-53(Al)-coated stainless steel fiber for efficient solid-phase microextraction of synthetic musks and organochlorine pesticides in water samples. *Anal Bioanal Chem* 409:5239–5247
- Zhang X, Ca J, Oakes KD, Breton F, Servos MR, Pawliszyn J (2009) Development of the space-resolved solid-phase microextraction technique and its application to biological matrices. *Anal Chem* 81:7349–7356
- Li Y, Wang Y, Zhang J, Sun C (2012) Determination of 16 polycyclic aromatic hydrocarbons in water using fluorinated polyaniline-based solid-phase microextraction coupled with gas chromatography. *Environ Monit Assess* 184:4345–4353
- Guo M, Song W, Wang T, Li Y, Wang X, Du X (2015) Phenyl-functionalization of titanium dioxide-nanosheets coating fabricated on a titanium wire for selective solid-phase microextraction of polycyclic aromatic hydrocarbons from environment water samples. *Talanta* 144:998–1006
- Yang L, Zhang J, Zhao F, Zeng B (2016) Electrodeposition of self-assembled poly(3,4-ethylenedioxythiophene) @gold nanoparticles on stainless steel wires for the headspace solid-phase microextraction and gas chromatographic determination of several polycyclic aromatic hydrocarbons. *J Chromatogr A* 1471:80–86
- Pawliszyn J (1997) *Solid-phase microextraction: theory and practice*. Wiley, New York
- Wei Q, James SL (2005) A metal-organic gel used as a template for a porous organic polymer. *Chem Commun* 12:1555–1556
- Huang W, Liu N, Zhang X, Wu M, Tang L (2017) Metal organic framework g-C<sub>3</sub>N<sub>4</sub>/MIL-53(Fe) heterojunctions with enhanced photocatalytic activity for Cr(VI) reduction under visible light. *Appl Surf Sci* 425:107–116
- Guan Y, Shi J, Xia M, Zhang J, Pang Z, Marchetti A, Wang X, Cai J, Kong X (2017) Monodispersed ZIF-8 particles with enhanced performance for CO<sub>2</sub> adsorption and heterogeneous catalysis. *Appl Surf Sci* 423:349–353
- Yang X, Xu Q (2017) Bimetallic metal-organic frameworks for gas storage and separation. *Cryst Growth Des* 17:1450–1455
- Li B, Wen H, Zhou W, Chen B (2014) Porous metal-organic frameworks for gas storage and separation: what, how, and why? *J Phys Chem Lett* 5:3468–3479
- Levine DJ, Runčevski T, Kapelewski MT, Keitz BK, Oktawiec J, Reed DA, Mason JA, Jiang HZH, Colwell KA, Legendre CM, FitzGerald SA, Long JR (2016) Olsalazine-based metal-organic



- frameworks as biocompatible platforms for H<sub>2</sub> adsorption and drug delivery. *J Am Chem Soc* 138:10143–10150
28. Rojas S, Carmona FJ, Maldonado CR, Horcajada P, Hidalgo T, Serre C, Navarro JAR, Barea E (2016) Nanoscaled zinc pyrazolate metal–organic frameworks as drug-delivery systems. *Inorg Chem* 55:2650–2663
  29. Li Q, Wang X, Chen X, Wang M, Zhao R (2015) In situ hydrothermal growth of ytterbium-based metal–organic framework on stainless steel wire for solid-phase microextraction of polycyclic aromatic hydrocarbons from environmental samples. *J Chromatogr A* 1415:11–19
  30. Li Q, Wang L, Wang X, Wang M, Zhao R (2016) Magnetic metal–organic nanotubes: An adsorbent for magnetic solid-phase extraction of polychlorinated biphenyls from environmental and biological samples. *J Chromatogr A* 1449:39–47
  31. Gao S, Fan B, Feng R, Ye C, Wei X, Liu J, Bu X (2017) N-doped-carbon-coated Fe<sub>3</sub>O<sub>4</sub> from metal–organic framework as efficient electrocatalyst for ORR. *Nano Energy* 40:462–470
  32. Skobelev IY, Sorokin AB, Kovalenko KA, Fedin VP, Kholdeeva OA (2013) Solvent-free allylic oxidation of alkenes with O<sub>2</sub> mediated by Fe- and Cr-MIL-101. *J Catal* 298:61–69
  33. Shang H, Yang C, Yan X (2014) Metal–organic framework UiO-66 coated stainless steel fiber for solid-phase microextraction of phenols in water samples. *J Chromatogr A* 1357:165–171
  34. Gao J, Huang C, Lin Y, Tong P, Zhang L (2016) In situ solvothermal synthesis of metal–organic framework coated fiber for highly sensitive solid-phase microextraction of polycyclic aromatic hydrocarbons. *J Chromatogr A* 1436:1–8
  35. Cavka JH, Jakobsen S, Olsbye U, Guillou N, Lamberti C, Bordiga S, Lillerud KP (2008) A new zirconium inorganic building brick forming metal organic frameworks with exceptional stability. *J Am Chem Soc* 130:13850–13851
  36. USEPA (2015) National Recommended Water Quality Criteria. United States Environmental Protection Agency, Washington, DC
  37. Directive 2008/105/EC of the European Parliament and of the Council of 16 December 2008 on environmental quality standards in the field of water policy, amending and subsequently repealing Council Directives 82/176/EEC, 83/513/EEC, 84/156/EEC, 84/491/EEC, 86/280/EEC and amending Directive 2000/60/EC of the European Parliament and of the Council. *Off J Eur Union* 348:84–97
  38. Canadian Council of Ministers of the Environment (CCME) (2015) Canadian environmental quality guidelines